ELSEVIER

Polymer 40 (1999) 3545–3554

polymer

Effect of the surfactant blend composition on the properties of polymerizing acrylamide-based inverse-emulsions: characterization by small-angle neutron scattering and quasi-elastic light scattering

Andreas Renken*, David Hunkeler

Laboratory of Polymers and Biomaterials, Department of Chemistry, Swiss Federal Institute of Technology, CH-1015 Lausanne, Switzerland

Received 12 January 1998; received in revised form 22 June 1998; accepted 14 July 1998

Abstract

In this study of the inverse-emulsion homopolymerization of acrylamide, surfactant blends of traditional fatty acid esters, ethoxylated fatty acid esters and ABA-type block copolymeric stabilizers were employed. Stable and transparent inverse latices with shelf lives of over one year were generated. Particle sizes were determined using quasi-elastic light scattering and small-angle neutron scattering and were found to be close to the threshold traditionally associated with microemulsions (100 nm). The turbidity of the polymer latices and the changes in viscosity during the polymerization are also similar to that observed in inverse-microemulsions. The radii of gyration calculated from SANS data were observed to be consistent with the hydrodynamic radius determined by QELS for the final polymerized products. SANS measurements of the inverse-emulsions at different reaction coordinates revealed a decrease in droplet diameters with conversion, with particles best described using a polydisperse spherical core + shell model. The decrease in droplet diameter with conversion has been attributed to a surfactant rearrangement in the interfacial sheath due to the consumption of surface active acrylamide.

Keywords: Acrylamide; Copolymeric surfactants; Inverse-emulsion

1. Introduction

Acrylamide based homo- and copolymers represent an important portion of the water-soluble polymer and hydrocolloid markets [1]. They are also applied in technologies such as flocculation, stabilization and dispersion [2]. Pulp retention in the paper industry [3], electrophoresis, water modification and the controlled release of urea for soil fertilization [4] represent other commercial uses. Permselective membranes for drug release [5] and beads for selective protein recognition [6] are emerging markets for acrylamide based biomaterials.

The synthesis of acrylic water-soluble polymers, in solution, is generally non-viable industrially, with the exception of catering to local markets where transportation costs are not a factor, due to extreme viscosities caused by the high molecular weights produced. This leads to heat transfer and reactor control limitations. Indeed, the enthalpy of polymerization of acrylamide ($\Delta H_p = 81.6$ kJ/mol) exceeds that of all other commodity monomers. Inverse-emulsion polymerization, first proposed in 1962 by Vanderhoff and co-workers [7,8], is a commonly used alternative for the production of acrylamide-based homo- and copolymers, though other heterogeneous processes such as precipitation [9] and sol–gel techniques are also employed. An extensive kinetic investigation of polymerizations in a heterophase water-in-oil system was carried out by Baade and Reichert [10]. Hunkeler proposed the first kinetic model of an inverse-macroemulsion [11]. It was subsequently shown, that the chemistry is specific to the monomer–emulsion–initiator–continuous phase system employed and is influenced by the structure of the dispersion [12].

1.1. Types of heterophase water-in-oil polymerizations

Inverse-emulsion polymerizations involve the dispersion of an aqueous monomer solution in a continuous aliphatic phase under continuous agitation. Non-ionic emulsifier blends are added to the organic phase at levels such that the overall hydrophilic–lipohilic balance (HLB) is between 3 and 8 [13]. Inverse-macroemulsions are kinetically stable and turbid systems with particle diameters generally

* Corresponding author.

0032-3861/99/$ - see front matter
PII: S0032-3861(98)00559-X

exceeding 150 nm, whereas inverse-microemulsions are thermodynamically stable, transparent latices, with particle sizes below approximately 100 nm [14,15]. One advantage of the smaller water-in-oil colloids is the ability of preformed polymer inverse-microemulsions to undergo chemical modification for example via a Manich reaction [16]. Furthermore, the thermodynamic stability of inverse-microemulsions avoids the need for periodic mixing which is required during the long-term storage of inverse-macroemulsions. The polymerization in inverse microlaticies often leads to very high-molecular weight products with good rheological properties such as high fluidity even at large volume fractions [15]. However, the high levels of emulsifier ($\geq$8% of the weight of the total emulsion) needed to obtain small droplet diameters is a clear disadvantage of inverse-microemulsion polymerization.

The mechanism of polymerizations in inverse-microemulsion includes droplet collision or migration of monomer through the interface into the droplets. The final product is composed of one single highly collapsed polymer chain per latex and an increase in droplet diameter with conversion of acrylamide to polyacrylamide has been observed [17]. The copolymerization between a water-soluble (e.g. acrylamide) and an organic phase soluble (e.g. styrene) monomer at the interface has also been studied by viscosimetry [18].

In recent years, the use of stabilizer blends which combine the advantages of macroemulsions (low emulsifier concentrations) and microemulsions (small particle size and long shelf life), have been developed [19]. These emulsifier systems consist of block copolymeric stabilizers of the ABA-type, often in combination with fatty acid esters and ethoxylated fatty acid esters [20,21]. The behaviour of these 'hybrid' inverse-emulsions/inverse-microemulsions is particularly interesting when acrylamide is copolymerized with quaternary ammonium monomers. Indeed, the final latex particle size was shown to be a function of the initial comonomer composition [22].

The aim of the present study was to investigate the stability and the latex properties of an inverse-emulsion as a function of reaction coordinate during the homopolymerization of acrylamide. The composition and concentration of the surfactant blends prepared at various ratios of polyoxyethylene sorbitan trioleate, sorbitan sesquioleate and a triblock copolymeric surfactant was of primary interest.

Table 1
Experimental conditions

Run[a]	Block co-polymeric surfactant content (%)	Blend composition		Total surfactant employed (g)
		Sorbitan sesquioleate/ polyoxyethene sorb. trioleate[b] (g)	ABA block copolymer[c] [g]	
1-1	0.00	4.5011	0	4.5011
1-2	12.5	3.9367	0.5631	4.4998
1-3	37.5	2.8128	1.6881	4.5009
1-4[d]	50.0	2.2508	2.2497	4.5005
1-5	62.5	1.6863	2.8134	4.4997
1-6	75.0	1.1255	3.3749	4.5004
1-7	87.5	0.5622	3.9378	4.5000
1-8	100	0.0000	4.4991	4.4991
2-1	12.5	3.5004	0.5001	4.0005
2-2	25.0	3.0010	0.9987	3.9997
2-3	37.5	2.4994	1.4997	3.9991
2-4[d]	50.0	2.0001	2.0000	4.0001
2-5	62.5	1.5010	2.5002	4.0012
2-6	75.0	1.0001	3.0054	4.0055
2-7	87.5	0.5014	3.4995	4.0009
2-7	100	0.0000	3.9989	3.9989
3-1	12.5	3.0618	0.4367	3.4985
3-2	25.0	2.6248	0.8741	3.4989
3-3	37.7	2.1806	1.3201	3.5007
3-4	50.0	1.7512	1.7501	3.5013
3-5	62.5	1.3119	2.1874	3.4993
3-6	74.9	0.8759	2.6194	3.4953
3-7	87.5	0.4378	3.0627	3.5005
3-8	100	0.0000	3.5001	3.5001

[a] Initiator: 2,2′-azobis(4-methoxy-2,4-dimethylvaleronitrile), $T = 45 \pm 2$°C (see Section 2).
[b] A blend of 31.0 wt% polyoxyethylene sorbitan trioleate (Tween 85, ICI-Americas, Willmngton, DE) and 69.0 wt% sorbitan sesquioleate (Arlacel 83, ICI Americas) was used to obtain an HLB of 6.0.
[c] A triblock copolymeric stabilizer composed of poly(12-hydroxystearic acid) and polyethylene oxide (Hypermer HB-239, ICI-Americas).
[d] Experiments repeated for SANS measurements with benzoin isobuthyl ether as initiator.

2. Experimental

2.1. Surface active agents

An ABA comb-like triblock copolymeric stabilizer consisting of poly(12-hydroxystearic acid) as a hydrophobic moiety and polyethylene oxide as the hydrophilic head was obtained from ICI Americas (HB 239, Wilmington, DE). Polyoxyethylene sorbitan trioleate (Tween 85) and sorbitan sesquioleate (Arlacel 83) were also obtained from ICI Americas in peroxide-free forms. Stabilizer blends with a constant HLB value of approximately 6.0 were obtained. The precise HLB of the blend is indeterminate since the block copolymeric stabilizers have only a quoted HLB range [23].

2.2. Polymer synthesis

The polymerizations of monomeric acrylamide crystals (Cytec, Charlotte, NC) were performed in a double-jacketed 100 ml glass reactor. Type I reagent grade water with a resistivity $>18\ \mathrm{M\Omega\,cm}$ obtained through a series of deionization cartridges (Continental Water Systems, Nashville, TN) was employed. The organic phase was a narrow cut of isoparaffinic mixture (Isopar M, Exxon; supplied by ChemCentral, Nashville, TN). The water to organic phase ratio was 1:1 by weight. The monomer concentration was 50 wt% of aqueous phase for all experiments and the emulsifier blends were dissolved in the organic phase at concentrations varying from 3.5 to 4.5 wt% of the total reaction mass, with experimental conditions listed in Table 1. The two phases (oil/surfactants and water/acrylamide) were mixed in the reactor and continually purged with purified 99.99% nitrogen (AL Compressed Gas, Nashville, TN) to remove any residual oxygen, which could inhibit the radical polymerization. One milliliter of the chemical initiator 2,2′-azobis(4-methoxy-2,4-dimethylvaleronitrile) (V-70, Wako Chemicals USA, Richmond, VA) dissolved in acetone at 7 g/l was added to the reactor. After the initiation temperature of 30°C, the reaction temperature was permitted to increase adiabatically to a value of 45 ± 2°C and was maintained at this level until the end of the polymerization. The reaction time was 1.5 h for each run. The conversion was measured by h.p.l.c. following the method described in Ref. [24].

2.3. Experimental design

In order to permit the investigation of the effect of the surfactant blend composition on the latex stabilities, the temperature, HLB, monomer concentration and aqueous to organic phase ratio were maintained constant throughout all experiments (Table 1). In earlier studies [20,21], stable final latices were obtained with surfactant levels as low as 4 wt%. The polymerizations were therefore carried out at surfactant levels of 3.5, 4.0 and 4.5 wt% of the total reaction mass and the block copolymeric stabilizer composition was varied from no block copolymer to 100 wt% (only block copolymer) in the stabilizer blend at a constant HLB value of 6.0.

2.4. Stability and turbidity measurements

The stability of the final emulsion was estimated using an accelerated settling test. The volume percentage of oil separation, with regards to initial oil volume, following centrifugation at 3000 rpm for 14 h (Marathon 21K centrifuge, Fisher Scientific, Norcross, GA) was taken as the metric.

The turbidity of the polymerized samples was measured at 640 nm with a spectrophotometer (Spectronic 20, Spectronic Instruments, Rochester, NY). The results were expressed as the percent transmittance relative to filtered Isopar M.

2.5. Quasi-elastic light scattering

Particle diameters were estimated by quasi-elastic light scattering at 514 nm and an angle of 90°. Data were acquired for a period of 20 s. using a Brookhaven BI9000 correlator (Brookhaven Instruments, Holtsville, NY). Each inverse-emulsion sample was diluted in Isopar K (0.02 g/20 ml, Exxon, supplied by ChemCentral, Nashville, TN), agitated for period of 2 s, and immediately placed in the goniometer for measurement. For polydisperse systems, such as those investigated here, quasi-elastic light scattering provides an estimate of the volume-averaged diffusion coefficient (D_v), and the corresponding volume-averaged hydrodynamic radius via the Stokes–Einstein relation.

The intensity autocorrelation functions $G(t)$ of polymerized inverse-emulsions were obtained at two surfactant levels (4.0 and 4.5 wt%) and for various block-copolymeric stabilizer contents. The electric field autocorrelation function $g(t)$ is related to the intensity autocorrelation function, normalized by the experimental baseline $\langle n\rangle^2$, by the Siegert relation:

$$\frac{G(t)}{\langle n\rangle^2} = 1 + b\cdot\left|g(t)\right|^2 \tag{1}$$

where b is a constant (coherence factor) considered as adjustable parameter in the fitting procedure. Since we are dealing with polydisperse scattering systems, a Laplace transformation relates the field autocorrelation function with the continuous distribution of decay rates $w(\Gamma)$:

$$G(t) = \int w(\Gamma)\cdot\exp(-\Gamma\cdot t)\,\mathrm{d}\Gamma \tag{2}$$

To determine the average diffusion coefficient from the linear relationship $\langle\Gamma\rangle = Dq^2$, the integral has to be inverted. This is done by minimum least-square fitting using the CONTIN program which employs the constrained regularization method to solve the ill-posed problem and restrict

the solution to the simplest possible one (parsimony) [25]. In the high dilution limit, the mutual diffusion coefficient obtained by QELS can be identified to the translational diffusion coefficient which is related to the hydrodynamic radius of the particles with the Stokes–Einstein relation:

$$r_H = \frac{k_B T}{6\pi\eta D} \tag{3}$$

where k_B is Boltzmann's constant, T the absolute temperature and η the solvent viscosity. More detailed discussions about QELS may be found in Refs. [26,27].

To assure the validity of the high dilution assumption, the samples were highly diluted prior to measurement (~0.125% emulsion in pure organic phase). At these low concentrations, however, the emulsions are quite unstable and the acquisition time had to be minimal (~20 s) to prevent coalescence. The method was introduced by Hernandez-Barrajas and provided accurate results in similar surfactant systems [19]. To increase the precision, each value was obtained from an average of 10 identical measurements with differences between diameters determined using the calculated and measured baseline of less than 1%.

2.6. Small-angle neutron-scattering measurements

Small-angle neutron-scattering measurements were performed on the High Flux Isotope Reactor (HFIR) of the Oak Ridge National Laboratory (Oak Ridge, TN) at a neutron wavelength of 4.75 Å. The samples for the SANS analyses were prepared prior to measurements in the 100 ml stirred glass reactor. The reactions were initiated by u.v.-radiation using a long wave u.v.-lamp (Black-Ray, Model B100 AP, Upland, CA) and benzoin isobutyl ether (90%, Aldrich, Milwaukee, WI). The peak temperature of the reaction, 45 ± 2°C, was controlled by modulating the lamp intensity. In order to enhance the scattering length density of the aqueous reaction medium, deuterium oxide (99.5%, Aldrich) was used in place of water. The distance between the detector and the sample was fixed at 3.2 m, leading to high Q range measurements ($0.008 < 0.15$ Å^{-1}). The SANS studies were limited to reaction systems using 4.5 and 4.0 wt% of emulsifier blends containing 50 wt% of block copolymeric surfactant. In addition to the monomeric and polymerized emulsions, two other samples were analysed at intermediate conversions to observe a possible change in particle diameter and shape during reaction. These samples were kept on ice until the measurements were performed.

2.7. Small-angle neutron-scattering modeling

The scattering density of the core was taken as the sum of the individual contributions of acrylamide and D_2O multiplied by their molar ratios relative to D_2O. The scattering of the shell was calculated as the sum of the individual contributions of each of the hydrophilic parts of the surfactants

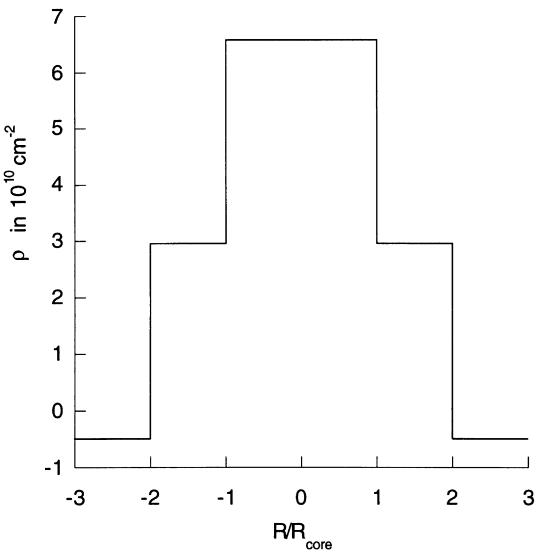

Fig. 1. Schematic representation of the scattering length density profile across the particle diameter. The values were calculated as outlined in the experimental section of this paper. $\rho_{core} = 6.5703 \times 10^{-10}$ cm^{-2}, $\rho_{shell} = 2.9512 \times 10^{-10}$ cm^{-2}, $\rho_{organic\ phase} = -4.9997 \times 10^{-11}$ cm^{-2}.

multiplied by their molar ratios relative to D_2O. The solvation of the core in the shell, i.e. the water (D_2O) present in the shell, was accounted for by assuming a water to emulsifier ratio of 10:1 in the surfactant layer. This value has shown to be a good estimate in preliminary experiments and previous studies [19]. The scattering density of the solvent was approximated as the scattering density of decane. The distribution of the scattering length density assumed in this study is illustrated in Fig. 1.

To separate the interparticle from the intraparticle contributions to the scattering density, the decoupling approximation is employed, i.e. it is assumed that there is no correlation between the position and the orientation of the latices [28–30]. This leads to a simple equation relating the scattered intensity $I(Q)$ to the form factor $\langle P(Q)^2\rangle$ which provides information regarding the shape, size and internal structure of the particle. The structure function $S(Q)$, arising from interparticle scattering, and the term $\Delta(Q)$[1], carrying information about deviations from sphericity and/or monodispersity, are also included in this basic equation [28]:

$$I(Q) = N\cdot\Delta(Q) + N\cdot\langle|P(Q)|\rangle^2\cdot S(Q) + B \tag{4}$$

where B is an additional background term, and N the particle number density. To obtain information from the $I(Q)$ *versus* Q data determined during SANS experiments, a particle shape is assumed leading to a determined particle form factor. For the case of strictly monodisperse spherical particles, $\Delta(Q) = 0$ and the particle form factor

[1] $\Delta(Q)$ is a root-mean-square term and is defined by: $\Delta(Q) = \langle P(Q)^2\rangle - \langle P(Q)\rangle^2$.

becomes:

$$P(Q,R) = 4\pi\cdot\left(R_1^3\left(\rho_c - \rho_s\right)\frac{\left(\sin\left(Q\cdot R_c\right) - Q\cdot R_c\cdot\cos\left(Q\cdot R_c\right)\right)}{\left(Q\cdot R_c\right)^3} + R_2^3\left(\rho_s - \rho_o\right)\frac{\left(\sin\left(Q\cdot R_s\right) - Q\cdot R_s\cdot\cos\left(Q\cdot R_s\right)\right)}{\left(Q\cdot R_s\right)^3}\right) \quad (5)$$

where R is the radius and ρ the scattering length density with the indices c, s and o for the core, shell and organic phase, respectively. The structure function $S(Q)$ is calculated assuming hard-spheres in the limiting case of vanishingly small external potential with the program by Hayter and Penfold [31]. In the case of ellipsoid particles, the decoupling approximation is only valid for diluted systems and the structure function was computed as before, assuming spherical particles of equivalent volume (mean spherical approximation). The form factor must account for all orientations of the micelles with respect to the neutron beam and is described in Ref. [32]. For the polydisperse spherical system, an exact analytical description avoiding the use of the decoupling approximation (Eq. (4)) has been derived assuming a Γ-distribution (Schulz distribution) [33,34]. However, in this study the mean spherical approximation has also been employed for this case since it described the data sufficiently well. The deviation from monodispersity ($\Delta(Q)$ in Eq. (4)) was calculated assuming a Schulz distribution, which is characterized by a breadth parameter $z_p = \left(1 - \left(\sigma/\bar{R}\right)^2\right)/\left(\sigma/\bar{R}\right)^2$, where σ is the variance of the distribution. The particle form factor for each particle size is described by Eq. (5) [32] and $\Delta(Q)$ is calculated using:

$$\left\langle |P(Q)|^2 \right\rangle = \int |P(Q,R)|^2 f(R)\, \mathrm{d}R \quad (6)$$

$$\left\langle |P(Q)| \right\rangle^2 = \left| \int P(Q,R) f(R)\, \mathrm{d}R \right|^2$$

where $f(R)$ is the Shulz distribution [34]. The structure function was again approximated by the $S(Q)$ of hard spheres of equivalent volume using the program of Hayter and Penfold [31].

3. Results

The dependence of the stability of polymerized inverse-emulsions on surfactant blend composition for total stabilizer concentrations of 3.5, 4.0 and 4.5 wt% is shown in Fig. 2. As expected, the stability of the inverse-emulsion increases with an increase in total emulsifier concentration. The optimal stability of the latices was observed for blends containing approximately 50 wt% block copolymeric stabilizer and was independent of the total surfactant concentration, over the tested range. This result is important since it provides a means of preparing stable inverse-emulsions of polyacrylamide with low total surfactant concentrations and avoids the use of high amounts of tri-block copolymeric stabilizers. Furthermore, the optimum is very flat, between 30 and 70% block-copolymer composition, permitting for an even lower block copolymeric stabilizer content with only limited loss in product quality. The remarkably long shelf life is reflected by the fact that some of the emulsions are still stable after more than 18 months without agitation as is seen on the photo in Fig. 3a. Traditional inverse-emulsions prepared from low-molecular weight diblock stabilizers show extensive phase separation after 2 months (Fig. 3b).

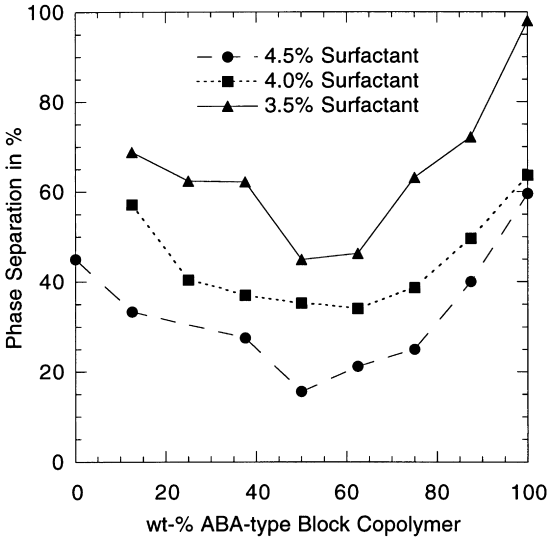

Fig. 2. Phase separation expressed as percentage of separated organic phase relative to the total organic phase volume as a function of the ABA-type triblock copolymeric stabilizer composition in the surfactant blends. The other stabilizers employed were polyoxyethylene sorbitan trioleate and sorbitan sesquioleate. The HLB of the surfactant blend was 6.0.

During the polymerization process, the turbidity was observed to change with conversion. Indeed, the initially turbid monomer emulsions became transparent following polymerization, as illustrated by the high transmittance of some polymerized samples (Fig. 4). Fig. 4 also shows the changes in turbidity and stability. The two curves (transmittance and reciprocal phase separation) show similar trends and are virtually parallel for the 4.5 wt% surfactant system, suggesting that a correlation between these two properties exists.

3.1. Particle size

The results of the QELS measurements are shown for 4.0 and 4.5 wt% surfactants in Fig. 5. The points are average values calculated from 10 repeated measurements ± 2 standard deviations. Clearly the minimal particle diameter is achieved at an ABA–block copolymer composition which corresponds to the most stable emulsion (50 wt%), as can be observed from a comparison with Fig. 2. The smallest particle size was 101 nm, close to the threshold

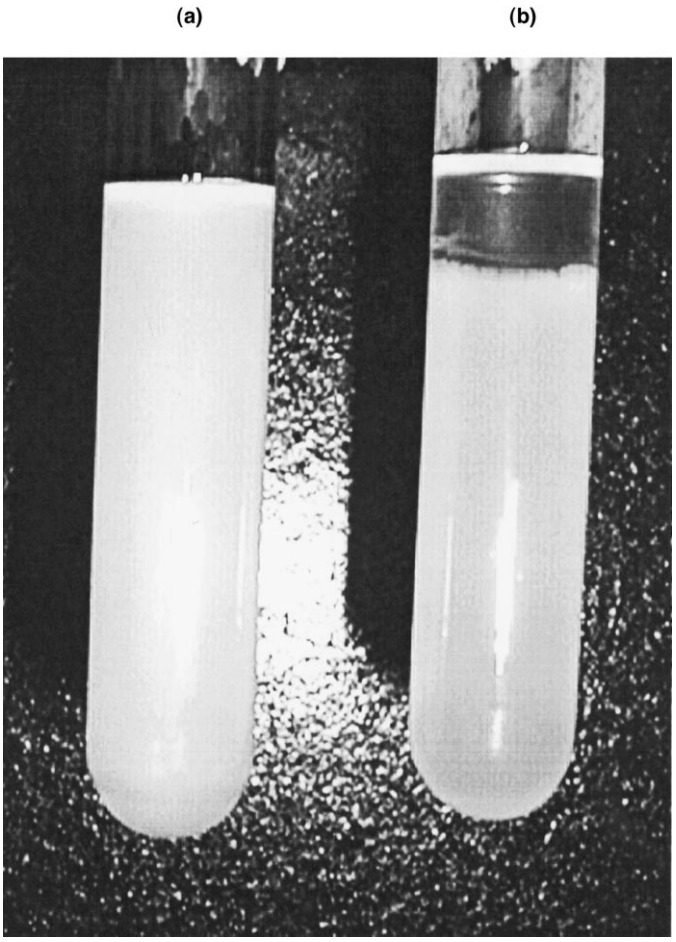

Fig. 3. Photos (a,b) showing the phase separation of polymerized inverse-emulsions after a period of 18 months for stabilizer blends with (a) and without (b) block copolymeric emulsifier. The block copolymeric stabilizer consisted of poly(12-hydroxystearic acid) and polyethylene oxide. The other surfactants employed were polyoxyethylene sorbitan trioleate and sorbitan sesquioleate. The HLB was set at a value of 6.0 and the total surfactant concentration was 4.5 wt%.

traditionally associated with inverse-microemulsions (100 nm). Therefore, while these water-in-oil systems have *not* evolved from thermodynamically stable inverse micelles, the final latices are able to mimic the properties of polymerized inverse-microemulsions.

3.2. SANS measurements

To obtain additional information regarding the evolution of particle size during the polymerization process, SANS measurements were performed on the initial monomer emulsions and on the final polymerized samples, as well as at two intermediate conversions. The intensity $I(Q)$ of the scattered neutron beam was measured as a function of the momentum transfer Q, and the spectra for the 4.5 wt% surfactant inverse-emulsion are shown in Fig. 6. The scattering intensities were measured after 8, 24 and 98 min[2]. This corresponds to approximately 20, 75 and 99% conversion.

[2] The turbidity abruptly fell after approximately 7 min, resulting in a very clear, transparent emulsion 2–3 min later.

The data (Fig. 6) show that the scattering pattern changes with conversion. This may be due to a change in particle shape, although a variation in the size of the inverse micelles due to conversion is more likely. At the high scattering angles at which the measurements were performed, no definite conclusion about the particle shape can be obtained. However, there does not appear to be any evidence of structural differences between the system observed at low and high conversions, indicating that the inverse-emulsion does *not* proceed through a bicontinuous inverse-microemulsion at intermediate stages during polymerization, as is the case for certain inverse-microemulsions studied by Candau et al. [35]. This is substantiated by the phase diagram in Fig. 7. This was obtained by adding acrylamide/water droplets to the organic phase containing the surfactants until the clear solutions turned turbid under strong agitation. Fig. 7 illustrates that the system under investigation is far from the inverse-microemulsion phase boundary irregardless of the surfactant blend ratio.

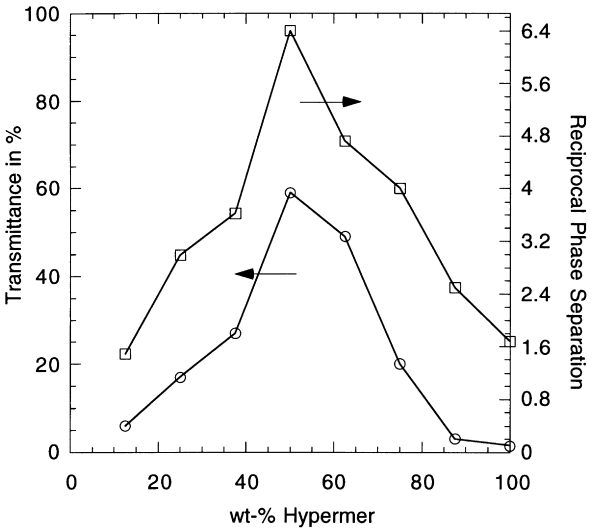

Fig. 4. Transmittance and reciprocal phase separation as a function of the percentage of ABA-type block copolymeric surfactant in the blend for a total emulsifier concentration of 4.5 wt%. The reciprocal oil separation is defined as 100/(phase separation in %). The transmittance was measured relative to pure filtered organic phase. The other stabilizers used were polyoxyethylene sorbitan trioleate and sorbitan sesquioleate while the HLB of the surfactant blend was 6.0.

3.3. SANS modeling

The particle size and shape were obtained through mathematical fitting of various particle characteristics to the measured intensity spectra. In this study, a polydisperse spherical core + shell model was found to describe the particles the most accurately, with χ-values between 9 and 16, as shown in Table 2. In contrast, the best least-squares fits to the data using an ellipsoidal monodisperse particle

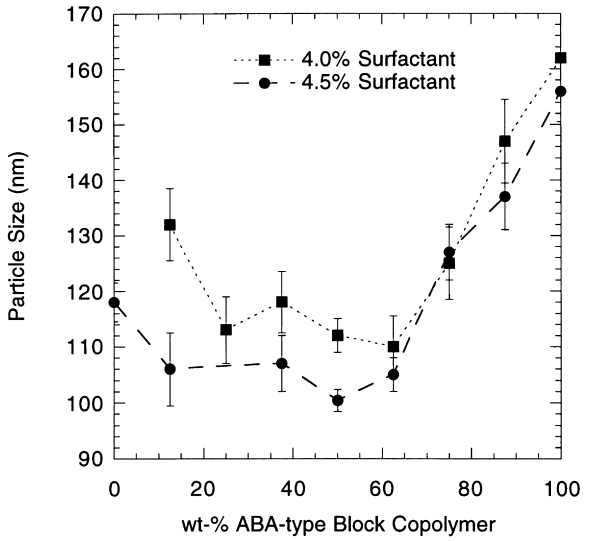

Fig. 5. Particle diameter (in nm) measured by QELS versus the percentage of ABA block copolymeric surfactant in the blend. The other stabilizers used were polyoxyethylene sorbitan trioleate and sorbitan sesquioleate while the HLB of the surfactant blend was 6.0. Each point represents the average of 10 identical measurements leading to the plotted error bars.

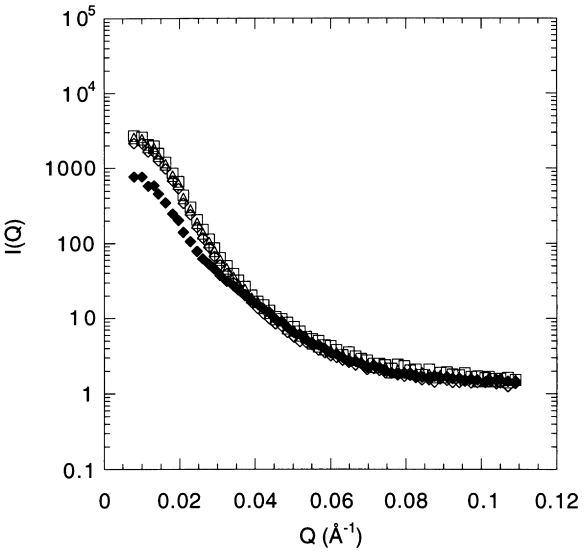

Fig. 6. SANS intensity spectra of polymerized inverse-emulsions prepared at a total surfactant concentration of 4.5 wt%. The emulsifier blend consisted of 50% ABA-type block copolymeric surfactant with 15.7 wt% polyoxyethylene sorbitan trioleate and 34.5 wt% sorbitan sesquioleate. Additional experimental conditions are described in the text. The intensity $I(Q)$ is plotted against the momentum transfer at various reaction coordinates: (♦) $t = 0$; (◇) $t = 8$ min; (△) $t = 24$ min; (□) $t = 90$ min (end of reaction).

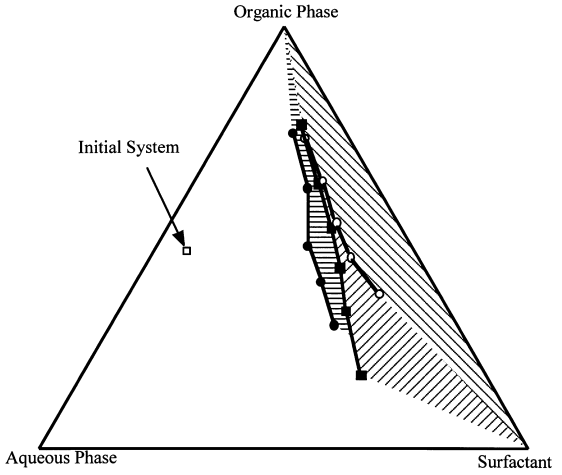

Fig. 7. Phase diagram for the acrylamide (50 wt%)/water:Isopar M:surfactant system. The surfactants were blends of sorbitan sesquioleate, polyoxyethylene sorbitan trioleate and poly(12-hydroxystearic acid)/polyethylene ABA block copolymer at HLB values of 6.0. The curves indicate the microemulsion/macroemulsion phase boundaries for surfactant blends containing 100 wt% (●), 50 wt% (■) and 0.0 wt% (○) block copolymeric stabilizer. The shaded regions indicate the microemulsion domains for each stabilizer blend. Clearly, the initial system (□) is located far from the boundaries, in the macroemulsion domain.

model were unstable and the convergence was strongly dependent on starting values. In addition, χ values[3] between 28 and 39 were calculated and the model was therefore not accepted. A monodisperse solid sphere model was also

[3] χ^2 is a measure for the acuracy of the fit (smaller values indicate better fits) and is defined as (sum of squares of weighted residuals)/(number of points minus number of parameters plus 1).

Table 2
Results of the SANS and QELS measurements

Total surfactant (wt%)	Reaction time (min)	QELS	SANS				
		r_H (nm)	r_g (nm)	r_i (nm)	r_o (nm)	z_p (–)	χ (–)
4.0	0	—	58.5 ± 0.8	53.1	84.4	29.4	9.3
4.0	12	—	50.3 ± 3.1	40.6	74.7	21.1	13.6
4.0	33	—	46.7 ± 2.4	30.7	71.4	25.9	14.5
4.0	90	**56 ± 1.1**	**46.4 ± 2.3**	35.0	69.6	28.5	14.9
4.5	0	—	57.2 ± 1.5	52.0	82.5	22.4	16.1
4.5	8	—	48.0 ± 2.8	37.6	71.7	25.5	15.3
4.5	24	—	46.1 ± 2.3	34.7	69.2	28.8	15.5
4.5	90	**51 ± 1.0**	**45.3 ± 1.9**	33.6	68.3	31.2	15.9

The background parameter B (Eq. (4)) was set to 1.1 and the scattering density of the solvent was approximated as the scattering density of decane. The radius of gyration was calculated using Eq. (7). The error bars on the SANS measurements are given by the fitting error (difference between measured data and values claculated according to the model).

r_H, hydrodynamic radius; r_g, radius of gyration; r_i, inner radius (core); r_o, outer radius (core + shell); z_p, polydispersity according to a Schulz (Γ) distribution.

rejected ($\chi > 54$) since it did not describe the data in the tested Q range ($0.008 < 0.15$ Å^{-1}) and predicted an oscillating pattern.

A comparison of the diameters measured by SANS and by QELS is presented in Table 2. Although the results obtained by QELS are smaller than the outer SANS radii, the particle sizes are similar ($r_i < r_H < r_o$). In fact, four different radii were determined: the hydrodynamic radius by QELS, the inner and outer radius (core and shell model) by SANS, and the radius of gyration r_g which was calculated for a hollow sphere from the SANS results. The latter is also shown in Table 2 and was computed using the following equation [36]:

$$r_g = \sqrt{\frac{2}{5} \cdot \frac{r_o^5 - r_i^5}{r_o^3 - r_i^3}} \tag{7}$$

As has been described, QELS provides volume-averaged radii, whereas SANS is based on number-averages. Therefore, a direct comparison between the results is not straightforward. However, the hydrodynamic radius (QELS) and the radius of gyration (SANS) of the final latices are within 20% of each other which, considering they estimate different molecular dimensions, is quite reasonable.

The thickness of the shell, approximately 310–350 Å, is reasonable compared to the shell thickness obtained in earlier studies by Hernández-Barajas [19], where only short-tailed polyoxyethylene sorbitan hexaoleate and sorbitan sesquioleate surfactants were employed.

4. Discussion

Fig. 8 shows the graphic results of the regression for a polydisperse spherical core + shell model to the SANS data for the 4.0 wt% surfactant monomer and polymer inverse-emulsions. The computed curves fit the experimental data well, as expressed by the χ values in Table 2, although some deviation in the intermediate to high Q range can be seen on the graphic. This is likely due to the approximations outlined in Section 2, and to the assumption of a sharp boundary layer model, i.e. the interpenetration of organic and water phase within the hydrophobic and hydrophilic parts of the surfactant, respectively, was not taken into account. Recently a new model including the diffuseness of the amphiphilic film has been derived and shown to provide better prediction of experimental data at high Q values [37]. However, the numerical values for the polydispersity and radii were not found to be significantly different. The accuracy of the sharp boundary model was therefore estimated to be sufficient for the current investigation.

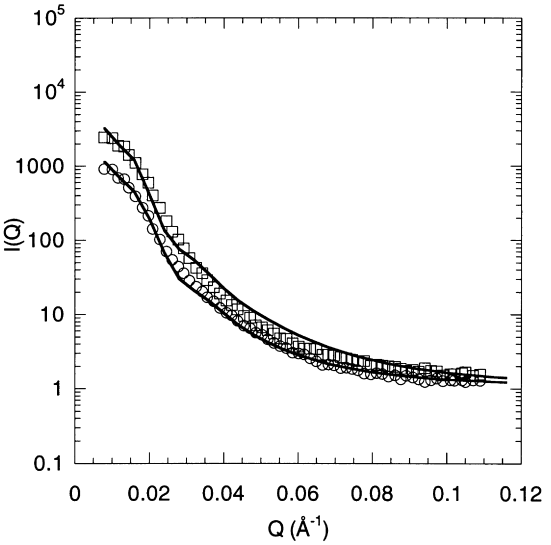

Fig. 8. SANS modeling showing the measured data and the computed curves using a polydisperse spherical core + shell model with a Schulz (γ) distribution. The total surfactant concentration was 4.0 wt% and the emulsifier blend contained 50 wt% ABA-type block copolymeric surfactant, 15.7 wt% polyoxyethylene sorbitan trioleate and 34.3 wt% sorbitan sesquioleate. Additional experimental conditions are described in the text. (□) Polymer emulsion; (○) monomer emulsion; (——) polydisperse spherical model.

The results shown in Table 2 are surprising in one regard as they indicate a lowering of the particle diameter by approximately 18% as a function of conversion. The decrease in droplet diameter essentially occurs at low conversions, below approximately 25%. Furthermore, the polydispersity, as estimated by the parameter z_p, does *not* increase significantly with polymerization which implies that a droplet break-up during the polymerization process is unlikely. A z_p value below 15 is characteristic for polydisperse systems, whereas systems with polydispersity greater 15–20 are essentially monodisperse (Triolo R, personal communication, July 15, 1997). The computed polydispersities indicate a relatively narrow particle size distribution, though not a strictly monodisperse system. This therefore excludes the presence of small colloids such as inverse-micelles during the polymerization. The unexpected trend in particle size with conversion could be explained by three phenomena:

(1) the higher density of the polymer as compared to the acrylamide monomer (1.122 g/cm^3 for acrylamide and 1.302 g/cm^3 for polyacrylamide [38]);

(2) a change in the average size of the extended interfacial sheath due to an emulsifier rearrangement to compensate for the surface active acrylamide which is consumed and displaced during the reaction;

(3) a shift of the inverse-microemulsion domain to engulf the initial system due to the local heat production at low conversions in the droplets [39].

The authors of this paper favour the first two explanations for the following reasons. The higher density of the polymer is equivalent to a lower specific volume and may partly explain the shrinking of the droplets. This effect accounts for a continuous decrease in particle diameter with conversion and cannot, therefore, explain the very steep decrease observed at low conversions. However, to compensate for the consumption of surface-active acrylamide during the reaction, sorbitan sesquioleate transfers from the bulk to the interface. The absence of the interfacial monomer lowers the optimal HLB required for stabilization [40], hence the ratio of sorbitan sesquioleate to polyoxyethylene trioleate at the boundary changes in favour of the fatty acid ester. This results in a denser interfacial sheath due to the smaller size of the sorbitan sesquioleate, and therefore in smaller droplet diameters. This rearrangement of the interfacial sheath also explains that no stable emulsion could be obtained when using high blockcopolymeric stabilizer levels since the interface is, then, not flexible enough. The interfacial acrylamide is consumed at low reaction times since an oil-soluble initiator was used. This leads to the steep decrease in particle size at low conversions. Therefore, the transparency of the polymerized latices is *not* caused by an artifact due to a change in the refractive index with conversion, but, indeed, to a decrease in droplet diameter.

The phase diagram for the heterophase water-in-oil systems used in this study is shown in Fig. 7 for stabilizer systems containing 100 and 50 wt% blockcopolymeric stabilizer as well as sorbitan sesquioleate/polyoxyethylene sorbitan trioleate at an HLB of 6.0 in isolation. Clearly, while the block-copolymeric surfactant provides an improved stability, the initial systems investigated are far from the inverse-microemulsion/inverse-macroemulsion phase boundary. A shift of this boundary so as to engulf the initial point, as was observed in earlier studies during non-isothermal polymerizations in hybrid inverse-emulsion/inverse-microemulsion [39], is therefore improbable. The phase diagram illustrates that the syntheses described herein occur in the inverse-emulsion domain [12]; hybrid inverse-emulsion/inverse-microemulsion conditions would require the initial system to be located close to the phase boundary [39].

5. Conclusions

Stable, non-settling transparent polyacrylamide inverse-emulsions can be obtained by using a blend of ABA-type block copolymeric stabilizer and traditional fatty acid ester and ethoxylated fatty acid ester-based surfactants. A decrease in particle size to droplet diameters generally associated to inverse-microemulsions is observed to occur during the polymerization. Some macroscopic properties of the inverse latices obtained show typical inverse-microemulsion behaviour such as transparency and changes in viscosity during polymerization [40]. This implies that the emulsifier blend has the role of permitting an inverse-emulsion to mimic the properties of a thermodynamically stable inverse-microemulsion without the excess surfactant. The decrease in droplet diameter with conversion has been attributed to a surfactant rearrangement in the interfacial sheath due to the consumption of surface active acrylamide.

Acknowledgements

We wish to thank Drs. Raymond S. Farinato and Logan A. Jackson for their help in carrying out the SANS measurements at the Oak Ridge National Laboratory. We also wish to express our gratitude to Professor Roberto Triolo who provided valuable suggestions and discussions regarding the SANS modeling. We would also like to thank Cytec for the financial support of this project.

References

[1] Goin J. CEH Marketing Research Report 5820000 D-E SRI International, August 1991.
[2] Buchholz FL In: Elvers H, Hawkins S, Schulz G, editors. Ullman's encyclopedia of industrial chemistry. Weinheim, Germany: VCH, 1992.
[3] Xiao HN, Pelton R, Hamielec A. Tappi J 1996;79:129.
[4] Abraham J, Pillai VNR. J Appl Polym Sci 1996;60:2347.

[5] Shamlou S, Kennedy JP, Levy RP. J Biomed Mater Res 1997;35: 157.
[6] Hjerten S, Liao JL, Nakazato K, Wang Y, Zamaratskaia G, Zhang HX. Chromatographia 1997;44:227.
[7] Vanderhoff JW, Bradford EB, Tardowski HL, Schaffer JB, Wiley RM. Adv Chem Ser 1962;34:32.
[8] Vanderhoff JW, Weiley RM. US Patent 3 826 771, 1966.
[9] Goodrich C. DE Patent 1 595 727-B, 1975.
[10] Baade W, Reichert KH. Eur Polym J 1984;20:505.
[11] Hunkeler D. PhD Thesis, McMaster University, Hamilton, Ontario, Canada, 1990.
[12] Hunkeler D, Candau F, Pichot C, Hamielec AE, Xie TY, Barton J, Vaskova V, Guillot J, Dimonie MV, Reichert KH. Adv Polym Sci 1994;112:115.
[13] Graillat C, Lepais M, Pichot C. J Dispers Sci Technol 1990;11:455.
[14] Candau F. In: Candau F, Ottewill RH, editors. Scientific methods for the study of polymer colloids and their applications. Dordrecht: Kluwer Academic, 1990.
[15] Candau F. In: El-Nokaly MA, editor. Polymer association structures: microemulsions and liquid crystals. Washington, DC: American Chemical Society, 1989.
[16] Kozakiewicz JJ, Huang SY. US Patent 4,956,399, 1990.
[17] Candau F, Leong YS, Pouyet G, Candau S. J Colloid Interf Sci 1984;101:167.
[18] Barton J, Juranicova V. Macromol Chem Phys 1996;197:3177.
[19] Hernandez-Barajas J. PhD Thesis, Vanderbilt University, Nashville, TN, USA, 1996.
[20] Ni HF, Hunkeler D. J Dispers Sci Technol 1996;18:123.
[21] Ni H. PhD Thesis, Vanderbilt University, Nashville, TN, 1996.
[22] Hernandez-Barajas J, Hunkeler D. Polymer 1997;38:449.
[23] Material Safety Data Sheet, Hypermer B-239 Wilmington, DE: ICI Americas, 1991.
[24] Hernandez-Barajas J, Hunkeler D, Petro M. J Appl Polym Sci 1996;61:1325.
[25] Provencher SW. Comput Phys Commun 1982;27:229.
[26] Stepanek P. In: Brown W, editor. Dynamic light scattering: the method and some applications. Oxford: Oxford Science Publications, 1993.
[27] Stock RS, Ray WH. J Polym Sci Polym Phys Ed 1985;23: 1393.
[28] Triolo R, Caponietti E. In: Rutschelli F, Fontana M, Coppola R, editors. Industrial and technological applications of neutrons. Amsterdam: North Holland/Elsevier, 1992.
[29] Wignall GD. In: Mark JE, Eisenberg A, Graessley WW, Mandelkern L, Samulski ET, Koenig JL, Wignal GD, editors. Physical properties of polymers Washington, DC: ACS Chemical Society, 1993.
[30] Higgins JS, Benoît HC. Polymers and neutron scattering. Oxford: Oxford Science Publications, 1993.
[31] Hayter JB, Penfold J. Mol Phys 1981;42:109.
[32] Hayter JB. In: DeGiorgio V, Corti M, editors. Physics of amphiphiles: miselles, vesicles and microemulsions. Amsterdam: North Holland, 1985.
[33] Griffith WL, Triolo R, Compere AL. Phys Rev 1986;A33:2197.
[34] Griffith WL, Triolo R, Compere AL. Phys Rev 1987;A35:2200.
[35] Candau F, Zerkhnini Z, Durand J-P. J Colloid Interf Sci 1986;114:398.
[36] Rumpel G, Sonderhausen HG. In: Beitz W, Küttner KH, editors. Dubbel: handbook of mechanical engineering. London: Springer Verlag, 1994.
[37] Gradzielski M, Langevin D, Magid L, Strey R. J Phys Chem 1995;99:13232.
[38] Chemistry of acrylamide. Wayne, NJ: American Cyanamid Company, 1969.
[39] Hernandez-Barajas J, Hunkeler D. Polymer 1997;38:5623.
[40] Candau F, Holtzscherer C. J Chim Phys 1985;82:691.